NANOSYSTEMS: PHYSICS, CHEMISTRY, MATHEMATICS, 2021, 12 (4), P. 505–511

Preparation and X-ray luminescence of $Ba_{4\pm x}Ce_{3\pm x}F_{17\pm x}$ solid solutions

D. S. Yasyrkina, S. V. Kuznetsov, A. A. Alexandrov, S. Kh. Batygov, V. V. Voronov, P. P. Fedorov

Prokhorov General Physics Institute of the Russian Academy of Sciences, Moscow, Russia

darya.yasyrkina@gmail.com

DOI 10.17586/2220-8054-2021-12-4-505-511

Single-phase BaF_2:Ce solid solutions containing 30 – 40 mol. % cerium with the simultaneous entry of potassium into the crystal lattice in an amount of 0.7 – 0.8 mol. % were prepared by coprecipitation from aqueous nitrate solutions with potassium fluoride as the fluoridating agent. The cerium X-ray luminescence intensity increases in response to increasing cerium concentration contrary to the concentration quenching effect.

Keywords: barium fluoride, cerium, X-ray luminescence.

Received: 21 July 2021

1. Introduction

Barium fluoride is a well-known heavy scintillator with two X-ray luminescence bands. The 220-nm band exhibits a very short decay time (0.8 ns), and a broad exciton band peaking around 300 nm has a decay time of 600 – 800 ns [1, 2]. In cerium-doped barium fluoride, exciton luminescence transforms to cerium ion luminescence induced by *d–f* electron transitions in Ce^{3+} ion [3–8]. The highest luminescence light yield occurs when the CeF_3 concentration is approximately 0.1 mol. %. At higher cerium concentrations, the luminescence intensity declines dramatically due to the concentration quenching phenomenon [9]. The decline was observed both for single crystals and for BaF_2:Ce^{3+} optical ceramics [10–15]. The concentration decay effect was assigned to defect cluster formation in fluorite-type lattices upon formation of $Ba_{1-x}Ce_xF_{2+x}$ solid solutions [9]. The composition corresponding to the highest luminescence light yield is the one with the highest concentration of free Ce^{3+}–F^- dipoles in the BaF_2 lattice [16]. In addition, barium fluoride dissolves up to 52 mol. % CeF_3, which radically changes the physical properties of its crystals, in particular, appreciably increases their density [17, 18].

A natural strategy to gain X-ray luminescence in high-cerium $Ba_{1-x}Ce_xF_{2+x}$ solid solutions is to destroy defect clusters to release Ce^{3+}–F^- free dipoles. This can be fulfilled by doping the solid solution with univalent cations, e.g., potassium. Potassium fluoride is frequently used to prepare precursors of fluoride optical ceramics [19–23]. It was due to the use of potassium fluoride in the synthesis of precursors that X-ray luminescence was induced in $BaCeF_5$ ceramics [24].

The goals of this work were to prepare $Ba_{1-x}Ce_xF_{2+x}$ solid solutions by coprecipitation from aqueous nitrate solutions with KF as the precipitating agent and to study X-ray luminescence of Ce^{3+} ions.

2. Experimental section

The initial reagents were used $Ce(NO_3)_3 \cdot 6H_2O$ (99.99% pure, Lanhit, Moscow, Russia), $Ba(NO_3)_2$ (specialty grade, Vekton, St. Petersburg, Russia), $KF{\cdot}2H_2O$ (reagent grade, the Fluoride Salts Plant, Russia), and bidistilled water. The potassium fluoride was stored in a desiccator. The reagents were used as received.

Samples were prepared by coprecipitation from aqueous solutions [25] by reaction (1):

$$(1-x)Ba(NO_3)_2+xCe(NO_3)_3\cdot 6H_2O+(2+x)KF\cdot 2H_2O = Ba_{1-x}Ce_xF_{2+x}\downarrow +(2+x)KNO_3+(10+2x)H_2O. \quad (1)$$

Barium nitrate and cerium nitrate solutions (0.08 mol/L each) were mixed, and the mixed solution was added drop by drop to a 0.16 M potassium fluoride solution under vigorous stirring on a magnetic stirrer. The potassium fluoride was used in a 7% excess over the stoichiometry. Once dropwise addition was over, the resulting suspension was stirred for 2 hours. After a precipitate settled, the mother solution was decanted, and the precipitate was washed with bidistilled water. Nitrate leaching was monitored by the diphenylamine test. The as-washed precipitate was air-dried at 45 °C. The cerium fluoride content in samples ranged from 30 to 55 mol. %. X-ray phase analysis of samples were carried out on Bruker D8 ADVANCE diffractometer using CuKα radiation. The unit cell parameters and coherent scattering domain (CSD) sizes were calculated in the TOPAS software ($R_{wp} < 10$). The size of the particles and the morphology of the samples were studied by means of Carl Zeiss NVision 40 scanning electron microscope (Germany) with an Oxford Instruments XMAX microprobe analyzer (UK) (80 mm^2) for energy dispersive X-ray spectroscopy. The particle size was averaged over 25 particles in the ImageJ software. The X-ray luminescence (XRL) spectra of the prepared samples were measured on a laboratory installation built of an X-ray source (tungsten anode) and an FSD-10 mini-spectrometer (Optofiber LLC, Moscow, Russia). A test sample was placed onto the holder horizontally under the beam of the X-ray source operating at a voltage of 40 kV and a current of 35 mA. The XRL signal was collected by a waveguide and transferred to the FSD-10 spectrometer. The luminescence was recorded in the 200 – 1000 nm range of the spectrum.

3. Results and discussion

Prior studies [26–29] imply that the coprecipitation of barium and cerium fluorides from aqueous solutions by various precipitating agents yields two-phase samples (pure barium fluoride and a fluorite phase containing 30 – 45 mol. % CeF_3). Single-phase samples can be prepared at 32–58 mol. % CeF_3 with hydrofluoric acid or ammonium fluoride as the precipitating agent [28].

X-ray diffraction patterns for samples with as-batch cerium concentrations of 30.0, 35.0, 40.0, 42.5, 45.0, 47.5, 50.0, and 55.0 mol. % shows on Fig. 1. X-ray diffraction experiments showed that our syntheses of solid solutions yielded single-phase powders with the fluorite structure containing 30 – 40 mol. % cerium. When the cerium concentration increased to 42.5 mol. %, a second (CeF_3-based) phase appeared, and its X-ray reflection intensity increased as the cerium concentration increased further (Fig. 1).

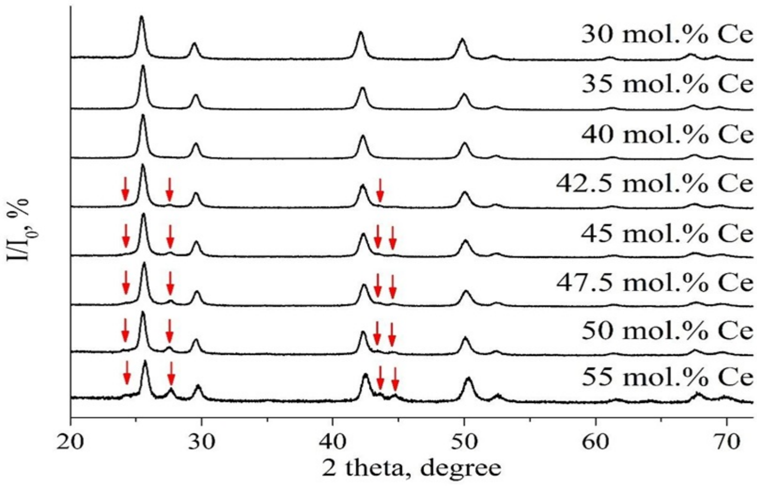

FIG. 1. X-ray diffraction patterns of BaF_2–CeF_3 samples with various cerium concentrations (the peaks marked with arrow refer to the CeF_3 tysonite phase)

Table 1 displays the calculated unit cell parameters and CSDs of prepared samples. An inspection of the tabulated values shows that, as the cerium concentration increases, the unit cell parameter of the fluorite phase decreases systematically due to the cerium radius being smaller than the barium radius [31].

The unit cell parameter versus rare-earth-ion concentration relationship for $Ba_{1-x}Ce_xF_{2+x}$ fluorite solid solutions borrowed from [30] was used to estimate the cerium concentration as

$$a = a_0 + kx, \tag{2}$$

where $a_0 = 6.2000$ Å is the BaF_2 unit cell parameter and $k = -0.36$ (Table 2). The estimated compositions were richer in cerium compared to the as-batch compositions for single-phase samples and were depleted in cerium for biphase samples.

Figure 2 shows the SEM images of single-phase samples. The mean particle sizes in these samples were 15 nm, in match with the CSD calculations (Table 1).

The EDX results reveals that potassium does enter the solid solution lattice when the as-batch cerium concentration is 35.0 or 40.0 mol. % (Table 2). Despite the additional entrance of potassium, there is a satisfactory match between the estimates by Eq. (2) and EDX measurements. Between the as-analyzed and as-batch concentrations, there is a reasonable match.

X-ray luminescence spectra for single-phase $Ba_{1-x}Ce_xF_{2+x}$ samples presented on Fig. 3.

An inspection of the X-ray luminescence spectra elucidated an increase in intensity of the 347-nm cerium luminescence in response to increasing cerium concentration.

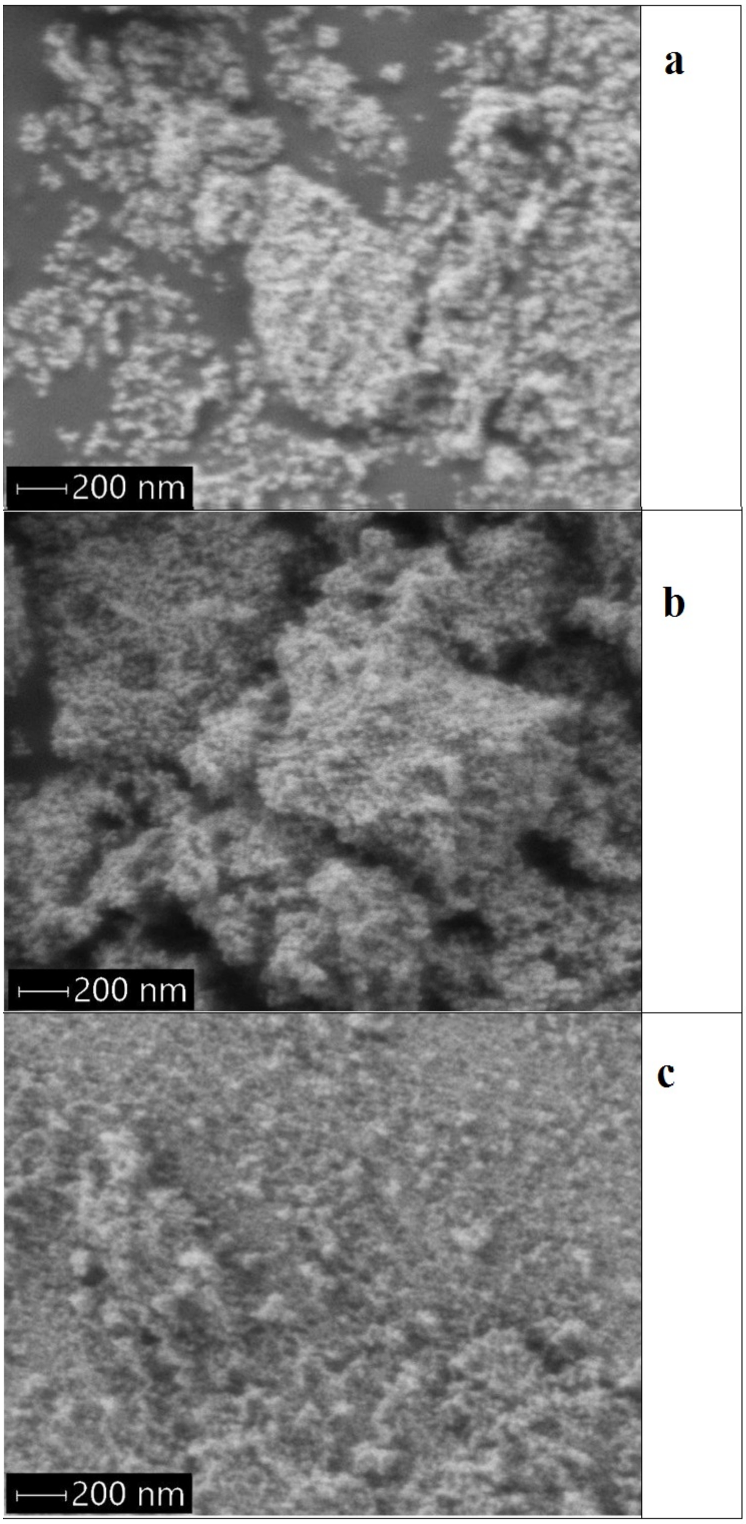

FIG. 2. SEM images of $Ba_{1-x}Ce_xF_{2+x}$ samples containing (a) 30.0 mol. %, (b) 35.0 mol. %, and (c) 40.0 mol. % nominal composition

TABLE 1. Unit cell parameters and CSDs of prepared samples

Nominal composition	Phase	Unit cell parameter, Å	CSD, nm
$Ba_{0.70}Ce_{0.30}F_{2.30}$	Fluorite	6.071(1)	18(1)
$Ba_{0.65}Ce_{0.35}F_{2.35}$	Fluorite	6.059(1)	19(1)
$Ba_{0.60}Ce_{0.40}F_{2.40}$	Fluorite	6.050(1)	17(1)
$Ba_{0.575}Ce_{0.425}F_{2.425}$	Fluorite	6.054(1)	16(1)
	presence a tysonite phase		
$Ba_{0.55}Ce_{0.45}F_{2.45}$	Fluorite	6.048(1)	16(1)
	presence a tysonite phase		
$Ba_{0.525}Ce_{0.475}F_{2.475}$	Fluorite	6.046(1)	16(1)
	presence a tysonite phase		
$Ba_{0.50}Ce_{0.50}F_{2.50}$	Fluorite	6.039(1)	15(1)
	presence a tysonite phase		
$Ba_{0.45}Ce_{0.55}F_{2.55}$	Fluorite	6.035(1)	15(1)
	presence a tysonite phase		

TABLE 2. Estimated compositions of prepared samples

Nominal composition	As calculated from the unit cell parameter	As probed by EDX
$Ba_{0.70}Ce_{0.30}F_{2.30}$	$Ba_{0.642}Ce_{0.358}F_{2.358}$	$Ba_{0.645}Ce_{0.355}F_{2.355}$
$Ba_{0.65}Ce_{0.35}F_{2.35}$	$Ba_{0.608}Ce_{0.392}F_{2.392}$	$Ba_{0.594}Ce_{0.398}K_{0.008}F_{2.390}$
$Ba_{0.60}Ce_{0.40}F_{2.40}$	$Ba_{0.583}Ce_{0.417}F_{2.417}$	$Ba_{0.563}Ce_{0.430}K_{0.007}F_{2.423}$
$Ba_{0.575}Ce_{0.425}F_{2.425}$	$Ba_{0.594}Ce_{0.406}F_{2.406}$	——
$Ba_{0.55}Ce_{0.45}F_{2.45}$	$Ba_{0.578}Ce_{0.422}F_{2.422}$	——
$Ba_{0.525}Ce_{0.475}F_{2.475}$	$Ba_{0.572}Ce_{0.428}F_{2.428}$	——
$Ba_{0.50}Ce_{0.50}F_{2.50}$	$Ba_{0.553}Ce_{0.447}F_{2.447}$	——
$Ba_{0.45}Ce_{0.55}F_{2.55}$	$Ba_{0.542}Ce_{0.458}F_{2.458}$	——

The unit cell parameter of the fluorite solid solution changes due to the interplay of two factors: the substitution of barium by a smaller cerium ion [31] and the entrance of an additional (interstitial) fluoride ion for providing charge compensation as

$$Ba^{2+} \to Ce^{3+} + F^{-}_{int} \tag{3}$$

Individual dipoles are observed only for low cerium concentrations in the solid solutions. The formation of *nnn* dipoles of trigonal symmetry is characteristic of low concentrations of cerium in the BaF_2 matrix [16, 32].

The association of dipoles in the barium fluoride matrix occurs with an increase in the cerium concentration, which leads to the formation of defect clusters. There is, as yet, no common structural description in terms of defect clusters for concentrated $Ba_{1-x}Ce_xF_{2+x}$ solid solutions in spite of numerous structural studies for chemically similar $Ba_{1-x}La_xF_{2+x}$ [33–40] solid solutions. An essential factor for a reliable interpretation of the results is the concentration range over which fluorite phases are formed in low-temperature syntheses of solid solutions in BaF_2–RF_3 systems. High-temperature syntheses in these systems yield ordered fluorite-related phases of $Ba_4R_3F_{17}$ stoichiometry [18, 42–45]. These phases were found in all BaF_2–RF_3 systems for R = Ce–Lu, Y when their phase equilibria were studied [18, 42, 46]. Kieser and Greis [46] prepared an ordered $Ba_4Ce_3F_{17}$ phase by heat-treating a disordered solid solution of the appropriate concentration at 400 °C. The fluorite-related $Ba_4R_3F_{17}$ phases are distinguished by a trigonal distortion of the fluorite-type lattice caused by spatial ordering of R_6F_{37} clusters [44]. Accordingly, the synthesis of single-phase fluorite solid solutions containing 30 – 40 mol. % cerium may be regarded as the synthesis of a $Ba_{4\pm x}Ce_{3\pm x}F_{17\pm x}$ phase, whose ordering is not manifested at the nanoscale level [47–51]. It is quite natural to suggest that R_6F_{37} clusters exist in the structure of this phase, substituting for parts of the Ba_6F_{32} lattice in accordance

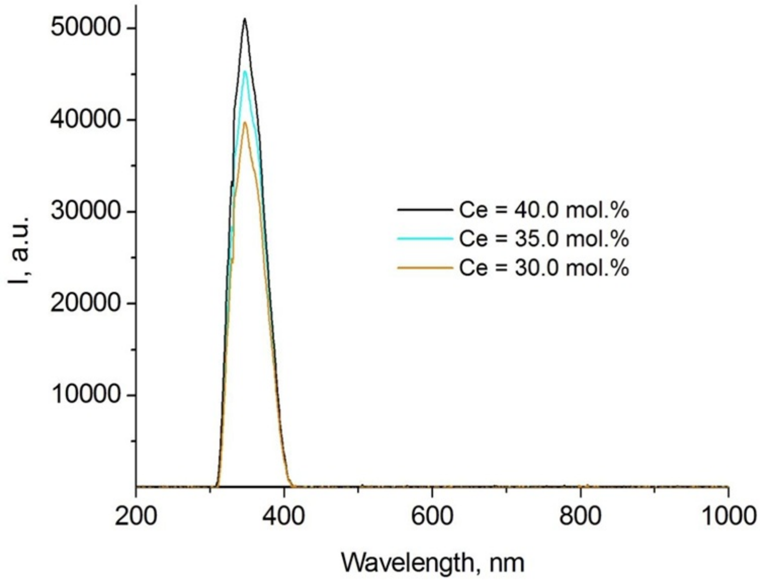

FIG. 3. X-ray luminescence spectra of single-phase $Ba_{1-x}Ce_xF_{2+x}$ solid solution samples

with the isomorphic substitution scheme advanced by Bevan et al. [52]. The shift of the X-ray luminescence peak from 330 to 347 nm may serve as an argument for this suggestion. The observation of X-ray luminescence in the prepared samples both by us and by Chen and Wu [24] may be regarded as the verification of the expected increase in free dipole concentration due to additional entrance of potassium in the barium fluoride host.

The concerted entrance of univalent and trivalent cations to form solid solutions is typical of the fluorite lattice [53]. Potassium was systematically observed to enter the host fluorite lattice in nanofluorides synthesized by coprecipitation of solid solutions [19]. In the NaF–BaF_2–GdF_3 ternary system, univalent sodium enters the lattice of the $Ba_4Gd_3F_{17}$ phase thereby extending its existence area [54].

4. Conclusions

A range of single-phase $Ba_{1-x}Ce_xF_{2+x}$ (x = 0.30 – 0.40) solid solutions, with an average particle size of 15 nm, prepared by coprecipitation from aqueous solutions, has been determined. It has been suggested that these solid solutions actually have a more complex composition, namely, $Ba_{4\pm x}Ce_{3\pm x}F_{17\pm x}$. The X-ray luminescence intensity in the solid solution samples increased in response to cerium concentration, increasing from 30 to 40 mol. % without concentration quenching. The absence of concentration decay was most likely due to potassium (0.7 – 0.8 mol. %) entering the crystal lattice, and thus, precluding cerium-based cluster formation.

References

[1] Rodnyi P.A. Core-valence luminescence scintillators. *Radiat. Meas.*, 2004, **38**, P. 343–352.

[2] Seliverstov D.M., Demidenko A.A., Garibin E.A., Gain S.D., Gusev Yu. I., Fedorov P.P., Kosyanenko S.V., Mironov I.A., Osiko V.V., Rodnyi P.A., Smirnov A.N., Suvorov V.M. New fast scintillators on the base of BaF_2 crystals with increased light yield of 0.9 ns luminescence for TOF PET. *Nuclear Instruments and Methods in Physics Research*, 2012, **695**, P. 369–372.

[3] Visser R., Dorenbos P., van Eijk C.W.E., Meijerink A., Blasse G. Energy transfer processes involving different luminescence center in BaF_2:Ce. *J. Phys. Condens. Matter*, 1993, **5**, P. 1659–1680.

[4] Sobolev B.P. Multicomponent crystals based on heavy metal fluorides for radiation detectors. *Barcelona: Institut d'Estudis Catalans*, 1995, P. 265.

[5] Wojtowicz A.J., Szupryczynski P., Glodo J., Drozdowski W., Wisniewski D. Radioluminescence and recombination processes in BaF_2:Ce. *J. Phys.: Condens. Matter*, 2000, **12**, P. 4097–4124.

[6] van Eijk C.W.E., et.al. Inorganic-scintillator development. *Nucl. Instrum. Meth.: Phys. Res.*, 2001, **460**(1), P. 1–14.

[7] Dorenbos P., et al. The Effects of La^{3+} and Ce^{3+} Dopants on the Scintillation Properties of BaF_2 Crystals. *Radiat. Effects Defects Solids*, 2000, **119-121**(1), P. 87–92.

[8] Janus S., Wojtowicz A.J. Scintillation light yield of BaF_2:Ce. *Opt. Mater.*, 2009, **31**, P. 523–526.

[9] Batygov S.Kh., Fedorov P.P., Kuznetsov S.V., Osiko V.V. Luminescence of $Ba_{1-x}Ce_xF_{2+x}$:Ce^{3+} Crystals. *Doklady Physics*, 2016, **61**(1), P. 50–54.

[10] Rodnyi P.A., Gain S.D., Mironov I.A., Garibin E.A., Demidenko A.A., Seliverstov D.M., Gusev Yu.I., Fedorov P.P., Kuznetsov S.V. Spectral-kinetic characteristics of crystals and nanoceramics based on BaF_2 and BaF_2:Ce. *Phys. Solid State*, 2010, **52**(9), P. 1910–1914.

[11] Fedorov P.P., Ashurov M.Kh., Boboyarova Sh.G., Boibobeva S., Nuritdinov I., Garibin E.A., Kuznetsov S.V., Smirnov A.N. Absorption and Luminescence Spectra of CeF_3-Doped BaF_2 Single Crystals and Nanoceramics. *Inorganic Materials*, 2016, **52**(2), P. 213–217.

[12] Batygov S.Kh., Bolyasnikova L.S., Garibin E.A., Demidenko V.A., Doroshenko M.E., Dykelskii K.V., Luginina A.A., Osiko V.V., Fedorov P.P. BaF_2:Ce^{3+} scintillation ceramics. *Doklady Physics*, 2008, **53**(9), P.485–488.

[13] Fedorov P.P., Kuznetsov S.V., Osiko V.V. Elaboration of nanofluorides and ceramics for optical and laser applications. *Photonic and Electronic Properties of Fluoride Materials*, 2016, **513**, P. 7-31.

[14] Luginina A.A., Baranchikov A.E., Popov A.I., Fedorov P.P., Preparation of barium monohydrofluoride BaF_2HF from nitrate aqueous solutions. *Materials Res. Bull.*, 2014, **49**(1), P. 199–205.

[15] Luo J., Ye L., Xu J. Preparation and properties of Ce^{3+}:BaF_2 transparent ceramics by vacuum sintering. *J. Nanoscience and Nanotechnology*, 2016, **16**, P. 3985–3989.

[16] Fedorov P.P. Association of point defects in nonstoichiometric $M_{1-x}R_xF_{2+x}$ fluorite-type solid solutions. *Butll. Soc. Cat. Cien.*, 1991, **12**(2), P. 349–381.

[17] Sobolev B.P. The Rare Earth Trifluorides. P.2. Introduction to materials science of multicomponent metal fluoridecrystals. *Barcelona: Institut d'Estudis Catalans*, 2000, P. 460.

[18] Sobolev B.P., Tkachenko N.L. Phase diagrams of BaF_2-(Y, Ln)F_3 systems. *J. Less-Common Metals*, 1982, **85**(2), P. 155–170.

[19] Kuznetsov S.V., Aleksandrov A.A., Fedorov P.P. Optical Fluoride Nanoceramics. *Inorganic Materials*, 2021, **57**(6), P. 555–578.

[20] Liu Z., Jia M., Yi G., Mei B., Jing Q., Liu P. Fabrication and microstructure characterizations of transparent Er:CaF_2 composite ceramic. *J. Am. Ceram. Soc.*, 2019, **102**(1), P. 285–293.

[21] Li J., Chen X., Tang L., Li Y., Wu Y. Fabrication and properties of transparent Nd-doped BaF_2 ceramics. *J. Am. Ceram. Soc.*, 2019, **102**(1), P. 178–184.

[22] Yi G., Li W., Song J., Mei B., Zhou Z., Su L. Structural, spectroscopic and thermal properties of hot-pressed Nd:$(Ca_{0.94}Gd_{0.06})F_{2.06}$ transparent ceramics. *J. Eur. Ceram. Soc.*, 2018, **38**(9), P. 3240–3245.

[23] Zhou Z., Mei B., Song J., Li W., Yang Y., Yi G. Effects of Sr^{2+} content on microstructure and spectroscopic properties of Nd^{3+} doped $Ca_{1-x}Sr_xF_2$ transparent ceramics. *J. Alloys Compd.*, 2019, **811**, P. 152046.

[24] Chen X., Wu Y. High Concentration Ce^{3+} doped BaF_2 transparent ceramics, *J. Alloys Compd.*, 2020, **817**.

[25] Fedorov P.P., Kuznetsov S.V., Mayakova M.N., Voronov V.V., Ermakov R.P., Baranchikov A.E., Osiko V.V. Coprecipitation from aqueous solutions to prepare binary fluorides. *Russian J. Inorg. Chem.*, 2011, **56**(10), P. 1525–1531.

[26] Kuznetsov S.V., Fedorov P.P., Voronov V.V., Samarina K.S., Ermakov R.P., Osiko V.V., Synthesis of $Ba_4R_3F_{17}$ (R stands for Rare-Earth Elements) Powders and Transparent Compacts on Their Base. *Rus. J. Inorg. Chem.*, 2010, **55**(4), P. 484–493.

[27] Batygov S.Kh., Mayakova M.N., Kuznetsov S.V., Fedorov P.P., X-ray luminescence of BaF_2:Ce^{3+} powders. *Nanosystems: Physics, Chemistry, Mathematics*, 2014, **5**(6), P. 752–756.

[28] Mayakova M.N., Voronov V.V., Iskhakova L.D., Kuznetsov S.V., Fedorov P.P. Low-temperature phase formation in the BaF_2-CeF_3 system. *J. Fluorine Chem.*, 2016, **187**, P. 33–39.

[29] Fedorov P.P., Mayakova M.N., Kuznetsov S.V., Voronov V.V., Ermakov R.P., Samarina K.S., Popov A.I., Osiko V.V. Co-Precipitation of Yttrium and Barium Fluorides from Aqueous Solutions. *Mat. Res. Bull.*, 2012, **47**, P. 1794–1799.

[30] Fedorov P.P., Sobolev B.P. Concentration dependence of unit-cell parameters of phases $M_{1-x}R_xF_{2+x}$ with the fluorite structure. *Sov. Phys. Crystallogr.*, 1992, **37**(5), P. 651–656.

[31] Shannon R.D. Revised effective ionic radii and systematic studies of interatomic distances in halides and chalkogenides. *Acta Cryst.*, 1976, **32**, P. 751–767.

[32] Murin I.V., Gunsser W. Relaxation methods for the study of ion transport in halide systems. *Solid State Ionics*, 1992, **53-56**, P. 837–842.

[33] Den Hartog H.W., Langevoort J.C. Ionic thermal current of concentrated cubic solid solutions of SrF_2:LaF_3 and BaF_2:LaF_3. *Phys. Rev. B.*, 1981, **24**(6), P. 3547–3554.

[34] den Hartog H.W., Pen K.F., Meuldijk J. Defect structure and charge transport in solid solutions $Ba_{1-x}La_xF_{2+x}$. *Phys. Rev. B*, 1983, **28**(10), P. 6031–6040.

[35] Wapenaar K.E.D., Van Koesveld J.L., Schoonman J. Conductivity enhancement in fluorite-structured solid solutions. *Solid State Ionics*, 1981, **2**, P. 145–154.

[36] Andersen N.H., Clausen K.N., Kjems J.K., Schoonman J. A study of the disorder in heavily doped $Ba_{1-x}La_xF_{2+x}$ by neutron scattering, ionic conductivity and specific heat measurements. *J. Phys. C: Sol. St. Phys.*, 1986, **19**, P. 2377–2389.

[37] Alexandrov V.B., Otroshchenko L.P., Fykin L.E., Bydanov N.N., Sobolev B.P. Features of the defective structure of $Ba_{0.5}Ce_{0.5}F_{2.5}$ fluorite solid solution according to the neutronographic study of single crystals. *Cryst. Reports.*, 1989, **34**(6), P. 1997–1501 (in Russian).

[38] Otroshchenko L.P., Alexandrov V.B., Muradyan L.A., Sarin B.A., Sobolev B.P. Neutron diffraction study of the features of fluorine ions incorporsation into $Ba_{1-x}R_xF_{2+x}$ solid solutions. *Butll. Soc. Cat. Cien.*, 1991, **12**(2), P. 383–391.

[39] Sobolev B.P., Golubev A.M., Otroshchenko L.P. et.al. *Crystallography Rep.*, 2003, **48**(6), P. 1012.

[40] Aminov L.K., Kurkin I.N., Kurzin S.P., Gromov I.A., Mamin G.V., Rakhmatullin R.M. Detection of cuboctahedral clusters in mixed crystals by the EPR method. *Physics of the Solid State*, 2007, **49**(11), P. 1990–1993 (in Russian).

[41] Maksimov B.A., Solans Kh., Dudka A.P., Genkina E.A., Font-Badria M., Buchinskaya I.I., Loshmanov A.A., Golubev A.M., Simonov V.I., Font-Altaba M., Sobolev B.P. The Fluorite-matrix-based $Ba_4R_3F_{17}$ (R=Y, Yb) crystal structure. Ordering of cations and specific features of the anionic motif. *Crystallography Rep.*, 1996, **41**, P. 50–57.

[42] Sobolev B.P. The Rare Earth Trifluorides. P.1.The high temperature chemistry of the rare earth trifluorides. *Barcelona: Institut d'Estudis Catalans*, 2000, P. 520.

[43] Grover V., Arhary S.N., Patwe S.S.J., Tyagi A.K. Synthesis and characterization of $Ba_{1-x}Nd_xF_{2+x}$ ($0.00 \le x \le 1.00$). *Mat Res. Bull.*, 2003, **38**, P. 1101–1111.

[44] Zolotova K.N., Kolbanev I.V., Ardashnikova E.I., Abakumov A.M., Dolgikh V.A. Interactions in the NdF_3-Nd_2O_3-MF_2 (M=Ba, Sr) systems. *Russ. J. Inorg. Chem.*, 2011, **56**, P. 1623-1631.

[45] Fedorov P.P., Luginina A.A., Popov A.I. Transparent Oxyfluoride Glass Ceramics. *J. Fluorine Chem.*, 2015, **172**, P. 22–50.

[46] Kieser M., Greis O. Preparation and properties of fluorite-related superstructure phases $Ba_4RE_3F_{17}$ with RE = Ce-Nd, Sm-Lu, and Y. *Z. anorg. allg. Chem.*, 1980, **469**, P. 164–171.

[47] Karbowiak M., Cichos J., Does $BaYF_5$ nanocrystals exist? – The BaF_2-YF_3 solid solution revisited using photoluminescence spectroscopy. *J. Alloys Compd.*, 2016, **673**, P. 258–264.

[48] Kuznetsov S.V., Nizamutdinov A.S., Mayakova M.N., Voronov V.V., Madirov E.I., Khadiev A.R., Spassky D.A., Kamenskikh I.A., Yapryntsev A.D., Ivanov V.K., Marisov M.A., Semashko V.V., Fedorov P.P. Synthesis and down conversion of luminescence of $Ba_4Y_3F_{17}$:Yb:Pr solid solutions for photonics. *Nanosystems: Phys., Chem., Math.*, 2019, **10**(2), P. 190–198.

[49] Li T., Li Y., Luo R., Ning Zh., Zhao Y., Liu M., Lai X., Zhong Ch., Wang Ch., Zhang J., Bi J., Gao D. Novel $Ba(Gd_{1-x}Y_x)_{0.78}F_5$: 20 mol % Yb^{3+}, 2 mol % Tm^{3+}($0 \leqslant x \leqslant 1.0$) solid solution nanocrystals: A facile hydrothermal controlled synthesis, enhanced upconversion luminescent and paramagnetic properties. *J. Alloys Comp.*, 2018, **740**, P. 1204–1214.

[50] Nizamutdinov A.S., Kuznetsov S.V., Madirov E.I., Voronov V.V., Khadiev A.R., Yapryntsev A.D., Ivanov V.K., Semashko V.V., Fedorov P.P. UV to IR down-conversion luminescence in novel $Ba_4Y_3F_{17}$:Yb:Ce solar spectrum sensitizer for silicon solar cells. *Optical Materials*, 2020, **108**, P. 110185.

[51] Kuznetsov S.V., Nizamutdinov A.S., Madirov E.I., Voronov V.V., Tsoy K.S., Khadiev A.R., Yapryntsev A.D., Ivanov V.K, Kharintsev S.S., Semashko V.V. Near infrared down-conversion luminescence. of $Ba_4Y_3F_{17}$:Yb^{3+}:Eu^{3+} nanoparticles under ultraviolet excitation. *Nanosystems: Phys., Chem., Math.*, 2020, **11**(3), P. 316–323.

[52] Bevan D.J.M., Strahle J., Creis O. The crystal structure of tveitite, an ordered yttrofluorite mineral. *J. Solid State Chem*. 1982, **44**(1), P. 75–81.

[53] Rozhnova Yu. A., Kuznetsov S.V., Luginina A.A., Voronov V.V., Ryabova A.V., Pominova D.V.,Ermakov R.P., Usachev V.A., Kononenko N.E., Baranchikov A.E., Ivanov V.K., Fedorov P.P. New $Sr_{1-x-y}R_x(NH_4)_yF_{2+x-y}$ (R = Yb, Er) solid solution as precursor for high efficiency up-conversion luminophor and optical ceramics on the base of strontium fluoride. *MatChemPhys.*, 2016, **172**, P. 150–157.

[54] Pavlova L.N., Fedorov P.P., Ol'khovaya L.A., Ikrami D.D, Sobolev B.P. Ordering of heterovalent solid solution with the fluorite structure in the NaF-BaF_2-GdF_3 system. *Crystallogr. Rep.*, 1993, **38**(2), P. 221–224.